Algorithm development for automatic detection of progressive damage in tunnel cross-sectional geometry

Christopher Nuñez[1] and Marck Regalado[2]

[a]Faculty of Civil Engineering, National University of Engineering, Perú
E-mail : christopher.nunez.v@uni.pe, marck.regalado.e@uni.pe

Abstract

Accurate assessment of tunnel conditions is vital for ensuring long-term safety and structural integrity, particularly in weak rock masses with complex geological conditions. This study introduces a methodology to analyze tunnel deformation and potential damage using point cloud data acquired in 2019, 2022, and 2024 through terrestrial laser scanning (TLS). The datasets were processed to remove outliers, irrelevant elements, and internal features, resulting in a clean representation of the tunnel's geometry. A novel algorithm integrates point cloud segmentation, centerline alignment, and projection techniques to derive tunnel profiles and monitor structural changes over time. The results demonstrate TLS's effectiveness in capturing high-resolution data for ovalization monitoring, revealing a consistent reduction in cross-sectional area throughout the tunnel and a rightward shift in the 2024 profiles. This approach underscores the potential of TLS for precise structural monitoring and deformation analysis in challenging environments.

Keywords –

Tunnel; Point cloud; Open3D

1 Introduction

Tunnel stability continues to be a major challenge in civil engineering. Various technologies have been applied to optimize monitoring processes, guaranteeing stability and minimizing the probability of tunnel failure throughout its useful life [1], [2]. Failures threatening the safety of tunnels constructed in soft or weak rock masses often occur throughout their long-term service periods [1], [3], [4]. The deformation and failure of rock masses are primarily influenced by discontinuities, which play a crucial role in determining their mechanical properties and overall stability [5]. Additionally, the mechanical behavior of tunnel structures is shaped by a combination of internal and external factors. While historical structural performance is an internal factor, external loads, such as temperature variations and water pressure, significantly affect the long-term properties and stability of the structure [3].

Therefore, ensuring the safe operation of tunnels is essential, as tunnel structures are highly susceptible to disasters due to the complex geological conditions in which they are situated [3]. However, traditional long-term monitoring methods are expensive, time-consuming, and highly dependent on operator subjectivity. These methods usually rely on one-dimensional random sampling, focusing only on limited areas, which leads to the omission of critical details [6], [7]. Additionally, traditional measurement approaches require surveyors to directly access hazardous geological areas. Despite these efforts, there are regions that cannot be manually measured, and the inherent risks involved in such measurements remain a major concern [8].

To address these challenges, many companies have invested in remote sensing technologies, including light detection and ranging (LiDAR), terrestrial laser scanning (TLS), digital photogrammetry, and unmanned aerial vehicles (UAVs) with 3D reconstruction capabilities [5]. For tunnel applications, laser scanning and photogrammetry are commonly employed, as both offer distinct technical advantages and potential value [6]. Firstly, these technologies enable rapid scanning of rock masses, such as temporarily exposed tunnel faces, significantly reducing survey time. Secondly, they allow geologists to perform measurements without physically approaching the tunnel face, thereby enhancing the safety of survey operations [5]. Additionally, sensor-based continuous monitoring techniques and analysis models are increasingly utilized to ensure tunnel functionality and maintain structural integrity over time [2].

Terrestrial Laser Scanning (TLS) offers high resolution and accuracy, making it a reliable method for data acquisition, often surpassing photogrammetry in precision while maintaining flexible measurement distances adaptable to various scenarios. Unlike photogrammetry, TLS does not require a light source, making it particularly suitable for dark underground environments such as tunnels. Its applications extend beyond tunnel monitoring to include stratigraphic modeling, archaeological excavation, and ancient site exploration [5], [8]. In tunnel engineering, TLS is frequently employed for ovalization monitoring of shield tunnels, with results aligning closely with structural calculations. Additionally, advancements in laser scanning technology have enabled the development of 3D LiDAR point clouds, which have proven effective in monitoring tunnel displacements [9].

After obtaining the point cloud, it is essential to process the data to identify relevant features such as discontinuities. Automated algorithms typically rely on clustering techniques or region-growing approaches, operating on spherical local support regions and utilizing normal vectors to detect features. Clustering methods, such as k-means, fuzzy k-means, ISODATA, DBSCAN, and CFSFDP, often use parameters like dip angle and dip direction derived from normal vectors for discontinuity identification. Additionally, model fitting techniques, including the Hough Transform (HT), Random Sample Consensus (RANSAC), and Principal Component Analysis (PCA), are employed to construct geometric models and estimate optimal plane parameters, enabling precise feature extraction and analysis [5], [10].

In this research, several challenges were identified within the dataset, including outliers, the presence of elements inside the tunnel, and irregularities in the tunnel's shape. To address these issues, we propose an algorithm designed to analyze tunnel damage using point cloud data captured by a terrestrial laser scanner (TLS) over three different years.

The structure of this paper is as follows: Section 2 discusses the materials and methods used to acquire and process the point cloud datasets. Section 3 presents the results, including the extraction of tunnel profiles for each dataset and an analysis of their changes over time. Finally, Section 4 highlights the scientific contributions and conclusions of this study.

2 Materials and Methods

This study focused on a tunnel with vertical walls and an arched roof, located in the Peruvian jungle (see Fig. 1). The tunnel serves as a critical passageway for gas transmission pipelines, facilitating their traversal across mountainous terrain. The structure has an approximate height of 2.10m and a width of 2.50m. The internal profile of the tunnel is reinforced with a layer of shotcrete, providing structural stability and durability.

Figure 1. External view of the tunnel located in Peru.

2.1 Data Acquisition

The tunnel data were collected during three different years: 2019, 2022, and 2024. For the datasets from 2019 and 2022, a Leica C10 laser scanner was employed, while the most recent data from 2024 was acquired using a Trimble X7 3D laser scanner. Table 1 summarizes the technical specifications of the Trimble X7 scanner.

Table 1 Features of the Trimble X7 3D Laser Scanner

Features	Specification
Scan Speed	26,600 points/sec
Scanning Range	350m - 600m
Accuracy	2.5mm at 100m
Noise tolerance	1.5mm - 2.5mm

For data acquisition planning, given the tunnel's 300-meter length, data capture stations were placed every 5 meters. The laser scanner was positioned at a height of 1.8 meters to ensure the capture of all possible points, including those behind pipes. Although the tunnel had sufficient natural lighting, artificial lighting was used to enhance data quality (see Fig. 2).

Figure 2. Data acquisition process inside the tunnel.

After completing the data acquisition process, which required a single day of work with a team of three individuals, the collected data was processed using Trimble software to export the point cloud in .ptl format.

2.2 Data Processing

After data acquisition, the collected data was processed in Python due to its extensive libraries for point cloud data handling and analysis. The primary library utilized was Open3D, an open-source tool for 3D data processing [11]. This library provides robust functionality for working with various point cloud formats, making it a versatile choice for this study. The parameters for data processing were based on the tunnel's measurements, including its height and width, to accurately filter outlier points.

2.2.1 Importing data

The data from 2019 and 2022 were provided as .txt files. Using NumPy, these files were transformed into point clouds containing only positional data. For the 2024 dataset, it was necessary to identify the specific format of the point cloud before processing, in this was .pts.

Open3D provides two primary methods for creating a point cloud: tensors or geometry-based methods. In this study, the geometry-based approach was chosen as it offers a wider range of features for controlling and processing the point cloud effectively. Figure 3 illustrates the 2024 point cloud, visualized using Open3D.

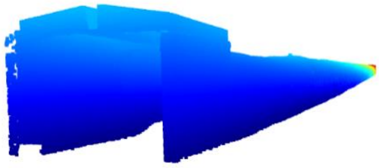

Figure 3. Visualization of the 2024-point cloud data processed in Open3D.

Finally, each dataset was uniformly downsampled using a specified voxel size. The points were grouped into voxels of 0.1m size, and each occupied voxel produced a single point by averaging all the points within it. Table 2 presents the results of the data import process.

Table 2 Summary of the Point Cloud Data

Year	Total points	Filtered Points	Retention Percentage
2019	70124628	348248	0.5%
2022	2259802	231868	10.26%
2024	4722696	208109	4.41%

Note: "Retention Percentage" represents the ratio of filtered points to total points, expressed as a percentage.

2.2.2 Cleaning data

As shown in Figure 3, the scanner captured points outside the tunnel, which are irrelevant to the objectives of this study. Similarly, within the tunnel, the presence of pipes required their removal, as the analysis focused solely on the contour profile. Additionally, several outlier points were identified during the scanning process. Figure 4 illustrates the interior of the tunnel, where the pipes and floor were captured.

Figure 4. The view of the tunnel's interior is represented in the point cloud.

To address these issues, a centerline representing the tunnel's overall geometry was first extracted. Subsequently, all points within a 1-meter distance from the centerline were removed. This process effectively eliminated the floor and the contour of the pipes from the point cloud (see Fig. 5). Next, the KDTree algorithm from the PyntCloud library was applied to identify neighboring points for each data point. Using this neighborhood information, the average distance from each point to its neighbors was computed. Points with an average distance greater than 0.20 meters were classified as outliers, and the corresponding neighboring points were eliminated. This iterative filtering process resulted in a clean point cloud that accurately represents the tunnel's contour shape.

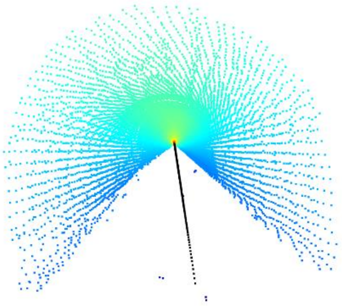

Figure 5. Point cloud after removing the floor and pipe shapes. The black line represents the centerline of the tunnel.

Then, Table 3 shows the number of points in each point cloud before and after the cleaning process, along with the corresponding percentage, which represents the ratio of points remaining after cleaning to the total points before cleaning.

Table 3. Summary of the point cloud data

Year	Downsampled points	Points after cleaning	Percentage
2019	348248	215646	61.9%
2022	231868	192832	83.2%
2024	208109	172915	83.1%

Since the structural movements are measured in millimeters, the focus is on removing outlier points generated near the tunnel floor. However, eliminating noise from the point cloud may impact the analysis of each section, as certain data points could be mistakenly discarded.

3 Results

3.1 Profiles

In this process, the centerline created during the data processing phase was divided into 2600 points. Using the direction of the line, a plane perpendicular to the line was created for each pair of adjacent points. This plane defined a region surrounding a specific number of points from each point cloud (see Fig. 6). With a voxel size of 0.10m, the minimum distance between each plane was also set to 0.10m.

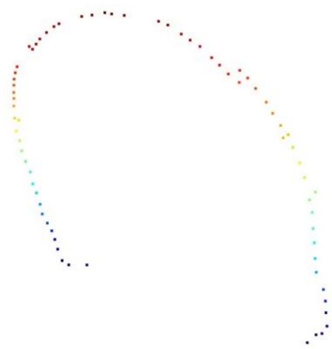

Fig. 6. Points in the surrounding region are defined by the perpendicular planes.

After extracting the points from each region, the projection of each point onto the plane perpendicular to the centerline was calculated. Using the Matplotlib library, a plane was generated with all these points connected by a line, forming the tunnel's contour (see Fig 7.).

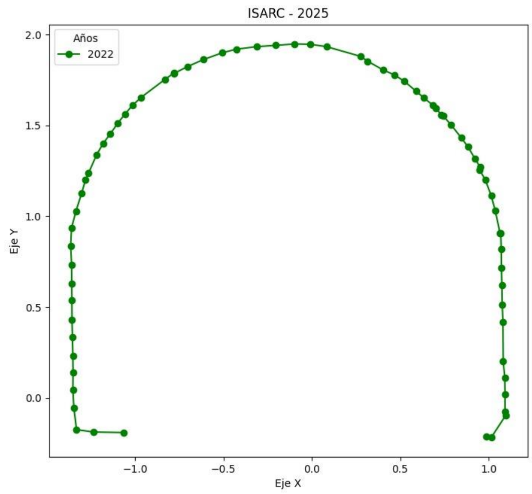

Fig. 7. Tunnel contour formed by points projected onto a plane perpendicular to the centerline.

Subsequently, all profiles were combined into a single 2D plane to analyze the variations in the tunnel's contour over time, highlighting changes observed across different years (see Fig. 8).

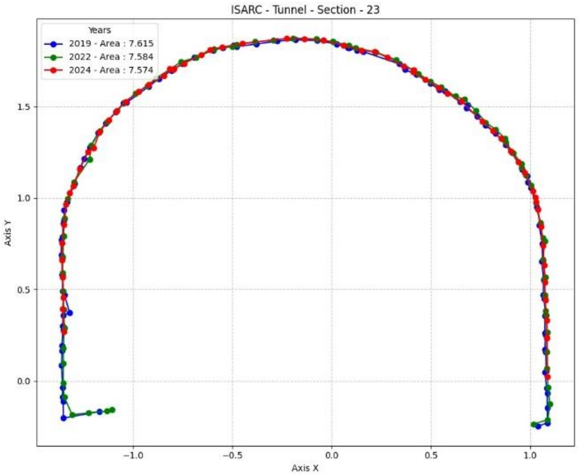

Fig. 7. Tunnel profiles from different years.

3.2 Damage identification

Using the three-point cloud datasets (2019, 2022, and 2024), each section was projected onto a 2D plane to analyze changes in the tunnel's cross-sectional area. Table 3 summarizes the reduction in area for a specific section, showing a consistent decrease over time. Additionally, the results indicate a reduction in tunnel width between 2019 and 2022 (see Fig. 8) and a consistent shift to the right across all sections over the years.

Table 4. Reduction in cross-sectional area

Year	Area (m2)	Percentage
2019	7.615	100%
2022	7.584	99.5%
2024	7.574	99.4%

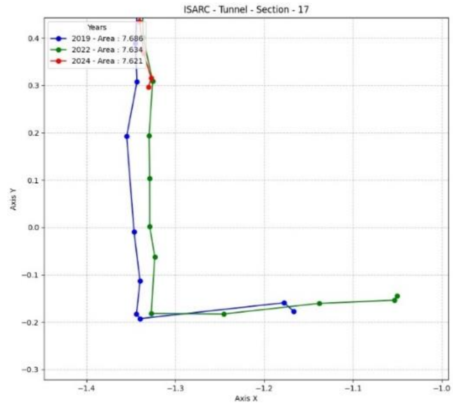

Fig. 8. Reduction observed in the lower-left section of the tunnel's cross-section.

An analysis was conducted along the entire tunnel, comparing cross-sectional areas from each year. The blue line represents the area from 2019, the green line corresponds to 2022, and the red line reflects 2024. The results reveal a noticeable reduction in the cross-sectional area of the tunnel over time, which may be attributed to ground movement or structural degradation of the tunnel. In Fig. 9, the comparison between 2019 and 2022 reveals noticeable changes in the tunnel's cross-sectional area, indicating structural modifications or deformation during this period. Similarly, Fig. 10 illustrates how the tunnel's sections in 2024 have shifted relative to 2022, showcasing continued changes over time

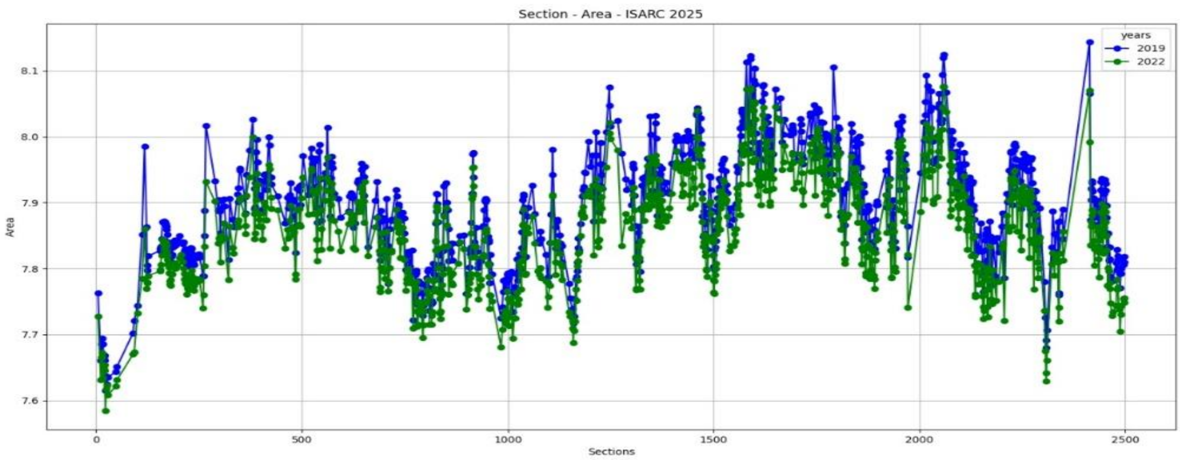

Fig. 9. Comparison of Tunnel Cross-Sections Between 2019 and 2022

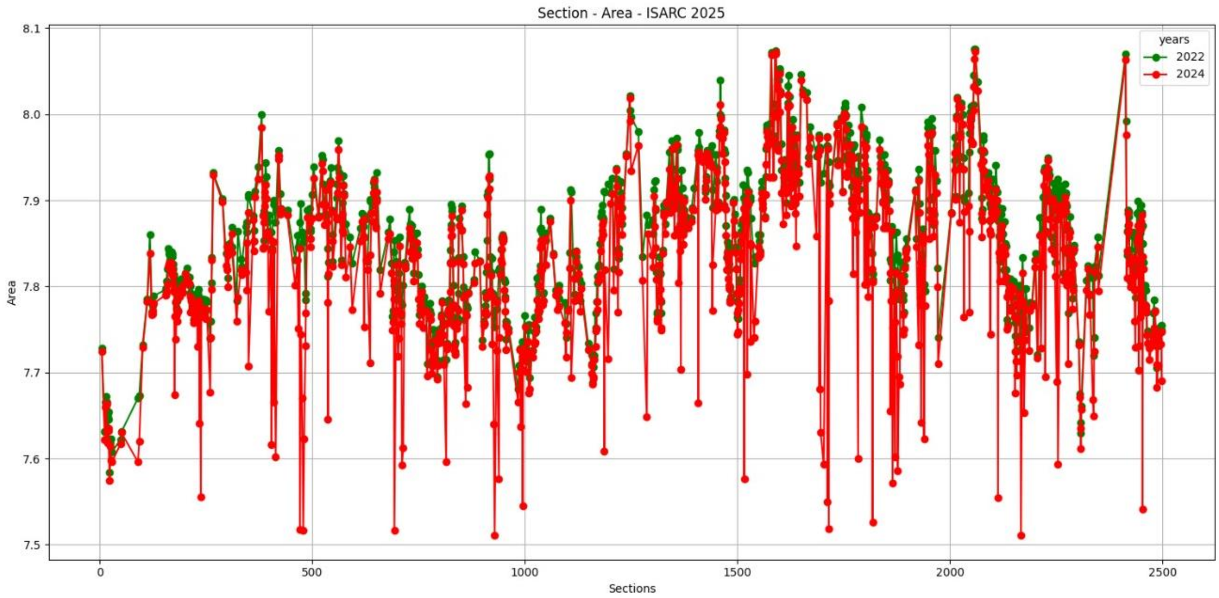

Fig. 10. Comparison of Tunnel Cross-Sections Between 2022 and 2024

4 Conclusions and Discussion

This study presents an innovative methodology for assessing tunnel deformation and structural changes over time using point cloud datasets acquired through terrestrial laser scanning (TLS) in 2019, 2022, and 2024. The following conclusions were derived:

- TLS has proven to be a reliable tool for capturing high-resolution data, facilitating detailed monitoring of the tunnel's structural changes. Its capacity to perform accurate measurements in challenging environments, such as dark underground tunnels, highlights its suitability for infrastructure assessment.
- Analysis of the tunnel profiles revealed a consistent reduction in cross-sectional area across all sections over the years. The results indicate a decline of 0.6% from 2019 to 2024, with notable deformation in specific regions, particularly the lower-left corner. This reduction may be attributed to geological movements or material degradation.
- A systematic rightward shift in the tunnel's cross-sections was observed over time. This movement underscores the need for continuous monitoring to identify and address potential instability risks associated with lateral displacement.
- The proposed algorithm effectively segmented the point cloud data, aligned it with the tunnel centerline, and projected profiles for comparative analysis. This approach enabled the detection of subtle changes in geometry, demonstrating its applicability for tunnel condition assessment.
- The findings highlight the importance of integrating advanced technologies, such as TLS and automated algorithms, into routine tunnel inspections. Such methods provide precise and actionable insights, reducing dependency on manual inspections and enhancing safety in hazardous conditions.

As observed, the findings have significant implications for structural monitoring and tunnel maintenance. Traditional tunnel monitoring techniques rely heavily on visual inspections, geodetic surveys and instrumentation-based systems. Although these methods have been widely used, they have limitations in terms of subjectivity, data resolution and safety. Visual inspections, for example, depend on the experience of engineers and can overlook subtle deformations. Geodetic surveys, which use total stations or leveling instruments, provide accurate measurements at discrete points, but require a lot of time and effort.

The progressive reduction of the cross-section indicates cumulative deformation that could compromise long-term stability. This problem could be due to the geomechanics of the area, such as ground movements, traffic loads in the area, or degradation of the tunnel materials. Early detection of deformations using TLS would allow engineers to implement preventive mitigation measures before critical failures occur. For instance, the use of metal trusses or increasing the thickness of shotcrete, the characteristics of which must be carefully calculated. On the other hand, being able to detect these changes in the cross-section is a better alternative compared to visual identification or manual measurements, which are subjective and depend on the experience of the inspector. Automating TLS reports makes it possible to generate reports, facilitating informed decision-making for tunnel maintenance.

References

[1] A. Sainoki, S. Tabata, H. S. Mitri, D. Fukuda, and J. ichi Kodama, "Time-dependent tunnel deformations in homogeneous and heterogeneous weak rock formations," *Comput Geotech*, vol. 92, pp. 186–200, Dec. 2017, doi: 10.1016/J.COMPGEO.2017.08.008.

[2] J. P. Yang, W. Z. Chen, M. Li, X. J. Tan, and J. xin Yu, "Structural health monitoring and analysis of an underwater TBM tunnel," *Tunnelling and Underground Space Technology*, vol. 82, pp. 235–247, Dec. 2018, doi: 10.1016/J.TUST.2018.08.053.

[3] X. Tan, W. Chen, T. Zou, J. Yang, and B. Du, "Real-time prediction of mechanical behaviors of underwater shield tunnel structure using machine learning method based on structural health monitoring data," *Journal of Rock Mechanics and Geotechnical Engineering*, vol. 15, no. 4, pp. 886–895, Apr. 2023, doi: 10.1016/J.JRMGE.2022.06.015.

[4] M. S. Kovačević, M. Bačić, K. Gavin, and I. Stipanović, "Assessment of long-term deformation of a tunnel in soft rock by utilizing particle swarm optimized neural network," *Tunnelling and Underground Space Technology*, vol. 110, p. 103838, Apr. 2021, doi: 10.1016/J.TUST.2021.103838.

[5] X. Peng, M. Wang, B. Huang, and P. Lin, "Efficient automated method for characterizing discontinuities in tunnel face rock mass point clouds," *Tunnelling and Underground Space Technology*, vol. 154, p. 106117, Dec. 2024, doi: 10.1016/J.TUST.2024.106117.

[6] H. Yang and X. Xu, "Structure monitoring and deformation analysis of tunnel structure," *Compos Struct*, vol. 276, p. 114565, Nov. 2021, doi: 10.1016/J.COMPSTRUCT.2021.114565.

[7] W. Mu, L. Li, D. Chen, S. Wang, and F. Xiao, "Long-term deformation and control structure of rheological tunnels based on numerical simulation and on-site monitoring," *Eng Fail Anal*, vol. 118, p. 104928, Dec. 2020, doi: 10.1016/J.ENGFAILANAL.2020.104928.

[8] J. wen Zhou, J. lin Chen, and H. bo Li, "An optimized fuzzy K-means clustering method for automated rock discontinuities extraction from point clouds," *International Journal of Rock Mechanics and Mining Sciences*, vol. 173, p. 105627, Jan. 2024, doi: 10.1016/J.IJRMMS.2023.105627.

[9] J. Li, F. Zhou, P. Zhou, J. Lin, Y. Jiang, and Z. Wang, "A health monitoring system for inverted arch of salt rock tunnel based on laser level deformation monitor and wFBG," *Measurement*, vol. 184, p. 109909, Nov. 2021, doi: 10.1016/J.MEASUREMENT.2021.109909.

[10] S. K. Singh, B. P. Banerjee, M. J. Lato, C. Sammut, and S. Raval, "Automated rock mass discontinuity set characterisation using amplitude and phase decomposition of point cloud data," *International Journal of Rock Mechanics and Mining Sciences*, vol. 152, p. 105072, Apr. 2022, doi: 10.1016/J.IJRMMS.2022.105072.

[11] Q.-Y. Zhou, J. Park, and V. Koltun, "Open3D: A Modern Library for 3D Data Processing," *arXiv:1801.09847*.